SynerCrete'18 International Conference on Interdisciplinary Approaches
for Cement-based Materials and Structural Concrete
24-26 October 2018, Funchal, Madeira Island, Portugal

MICROSTRUCTURE-BASED PREDICTION OF THERMAL PROPERTIES OF CEMENT PASTE AT EARLY AGES

Hadi Mazaheripour[(1)], Amin Abrishambaf[(1)], Rui Faria[(1)], Miguel Azenha[(2)], Guang Ye[(3)]

(1) Faculty of Engineering, University of Porto (FEUP), 4200-465 Porto, Portugal.
(2) School of Engineering, University of Minho, 4800-058 Guimarães, Portugal.
(3) Microlab, Delft University of Technology, Delft, The Netherlands.

Abstract

The time-dependent process of cement hydration affects many physical and mechanical properties of the cement-based materials, particularly at early ages. To estimate the thermomechanical response of cementitious composites, such as concrete, determination of thermal properties, including heat capacity, thermal conductivity and coefficient of thermal expansion, are necessary. An effort is made in the present study to predict the thermal behaviour of cement pastes by simulating the development of the microstructure during the hydration progress. The model deals with the thermal properties of main cement hydration products, Calcium-Silicate-Hydrate (C-S-H) and Calcium Hydroxide CH, and the change in their volume fraction in the microstructure. The paper discusses the results of thermal conductivity and the specific heat capacity from the model, and they are compared to some recent experimental data from the literature.

1. Introduction

The prediction of the thermomechanical behaviour of concrete depends on adequate knowledge of its thermal properties. Heat capacity, thermal conductivity and coefficient of thermal expansion are the properties that play important roles in the structural behaviour of concrete structures (RC) at early ages, especially the massive ones [1], which are particularly prone to significant thermal stress development. At early ages, these thermal properties evolve with the changes in the microstructure due to cement hydration processes. Therefore, an understanding of the thermal properties of cement paste can contribute to the prediction of such properties for concrete. The evolution of thermal properties in cement paste during hydration is mainly due to the difference between the thermal properties of the hydration product (i.e. Calcium-Silicate-Hydrate (C-S-H)) and those of the corresponding reactants. In this paper, a microstructural modelling strategy is proposed to estimate the thermal properties of cement paste at early age in respect with the change in the volume fraction of the cement paste components in the microstructure. The thermal properties of cement paste are simulated

by modelling its microstructure on a cubic representative elementary volume (REV) with a periodic boundary condition. The REV is obtained through application of the HYMOSTRUC3D hydration model. The method and some primary results in terms of the effective thermal conductivity and the specific heat capacity per unit mass are presented in the present herein.

2. Cement paste: properties and simulations of nano-micro structural features

This study focuses on CEM II 42.5R, as marketed in Portugal. The mineral composition of this cement, expressed in mass percentage, is: 63.2% C3S, 2.6% C2S, 7.6% C3A, 11.6% C4AF, and 11.3% limestone. The cumulative particle distribution size (PSD) of cement was measured by using Laser Diffraction Spectrometry (LDS). The PSD curves can be fairly defined as a Rosin-Rammler function, i.e. $f(D)=1-e^{-bDn}$, where D is the diameter of the cement particle, and b and n are coefficients. By employing a curve fitting analysis, the values of 0.052 and 1.00 were calculated for, respectively, b and n. The thermal properties of individual components of cement clinker and limestone, as well as the hydration product adopted from the literature, and written in Table 1.

Table 1. Some thermal properties of cement paste components used for the simulation

Compound		**Thermal conductivity** W/m.K	**Specific heat capacity** J/(kg.K)	**Density** g/cm^3
Clinker phases	C3S	3.45 [2]	0.69 [2]	3.13 [2]
	C2S	3.35 [2]	0.68 [2]	3.31 [2]
	Average	3.29	0.73	3.15
Limestone (saturated)		2.95 [3]	0.92 [3]	2.50 [3]
CH		1.32 [2]	1.15 [2]	2.17 [2]
C-S-H globules (Ca/Si=1.75)		0.98 [2]	0.84 [2]	2.6 [2]
Inner C-S-H – saturated *		0.870 [2] (0.883)	0.86-0.97 [2] (0.88)	2.18
Outer C-S-H– saturated *		0.825 [2] (0.830)	0.86-0.97 [2] (0.90)	1.99
Water in gel pores		0.607 [4]	1.13 [5]	1.0
Water in capillary pores		0.607 [4]	4.18	1.0

* the values in the parenthesis obtained from the nanostructure model in the present study.

2.1 Simulation of the nanostructure of C-S-H

The thermal conductivity and the specific heat capacity of the inner and outer C-S-H is estimated by simulating the nanostructure of these products. The nanostructure of outer C-S-H is constructed by assuming the random close packing of mono-sized (5 nm) C-S-H sphere globules (Figure 1a). The random close packing of mono-sized is equivalent to "*the maximum density that a large, random collection of spheres can attain and this density is a universal quantity*" [6]. This packing density of mono-sized sphere is about 0.64, which is very close to the packing density reported for the outer C-S-H globules [2]. In this study, the code from Skoge *et al.* [7] is used to generate the nanostructure of outer C-S-H, which is based on molecular dynamics mechanism. The nanostructure of the inner C-S-H is also simulated by the close packing of mono-sized (5 nm) C-S-H globules (Figure 1b). For the case of the inner C-S-H, the close packing of mono-sized spheres is arranged in a lattice, and not as a random

form. The packing density is approximate 0.74, which is higher than that of the random close packing, and it is very close to the density reported for the inner C-S-H in the literature [2].

2.2 Simulation of the microstructure of cement paste

The latest version of HYMOSTRUC3D software [8] is used for constructing the cement paste microstructure during hydration. This simulation is implemented in a cubic REV volume of the cement paste where the cement particles are modelled as spheres randomly distributed. The initial number and diameter of the particles are built in accordance with PSD curve. The main cement hydration products are the Calcium-Silicate-Hydrate (C-S-H) and the Calcium Hydroxide (CH). C-S-H is formed as two layers of inner and outer products, which are the result of the inward and outward radial growing of the cement spheres. The important parameters to be defined in HYMOSTRUC3D for modelling cement hydration are minimum and maximum size of the cement particles, REV size, temperature, *w/c*, and two reaction factors that control the speed and progress of hydration. For further details on fundamental aspects of the model parameters, the reader is addressed to the studies in [8, 9]. The hydration analysis was performed for *w/c*=0.3, 0.4, 0.5 and 0.6. The curing temperature was set at 20^{o}C. An image of the microstructure can be seen in Figure 1c.

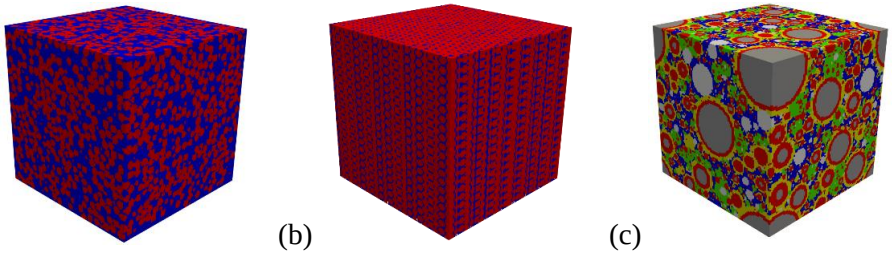

(a) (b) (c)

Figure 1. The nanostructure of (a) the outer CSH, and (b) the inner CSH (blue: gel water, red: CSH globules); (c) the microstructure of a hydrated cement paste (grey: unreacted cement, red: inner CSH, yellow: outer CSH, white: limestone, blue: capillary water, green: CH);

3. Estimation of the effective thermal properties

The REV microstructure obtained from HYMOSTRUC3D is digitalized by means of voxels of 1.0×1.0×1.0 μm^3. A single material phase is assigned for each voxel based on the greatest volume fraction of the material that the voxel is representing. For example, if the voxel is in the boundary of two material phases (e.g. inner and outer C-S-H), the voxel represents the material with the higher volume fraction. The whole REV is totally discretized to 10^6 voxels of six different material phases including: unreacted cement, inner and outer C-S-H, CH, limestone, and pore/water phases. The simulations assume saturated conditions (simplifying assumption at the present stage), hence the pore phases are filled by water, and they are simulated as solid-like behaviour elements with the relevant thermal conductivity. The simplification of solely considering thermal conduction effects for water is backed by previous studies, which have shown that the other contributions such as thermal convection and radiative conductivity in the pore phases (both capillary and gel pores) can be neglected at the microstructural scale [10]. The size of the pores is an effective parameter to address the thermal properties of water. Two types of water phases are assumed: 1) water in gel pores (being presented only in gel porosity in the nanostructure of C-S-H), and 2) water in capillary

pores (being presented in the microstructure of cement paste. The thermal properties of these two types of confined water are given in the last rows in Table 1, based on [2, 4]. The same strategy is followed for discretization of the nanostructure of the inner and outer C-S-H. In this case, the nanostructure includes only two material phases: 1) C-S-H globules; 2) gel pores.

The thermal conductivity: the thermal conductivity of C-S-H is estimated by simulating the discretised REV nanostructure of the outer and inner C-S-H under a steady state condition of temperature field. By imposing unit degree of temperature difference at two sides of the REV, the effective thermal conductivity simply is

$$\lambda_{eff} = -\left\langle q_z^r \right\rangle \Delta z = -\left\langle q_z^r \right\rangle L \tag{1}$$

where q_z^r is the heat flux of phase *r* flowing through the REV in *z* direction from the outer surface with higher temperature to another surface with lower temperature. The operator $\langle . \rangle$ denotes volume averaging. *L* is the length of the REV, in correspondence to the distance between the two surfaces with a unit degree of temperature difference. The discretised REV is imported to DIANA FEA software. The voxels are considered as eight-node isoparametric solid elements for general three-dimensional potential flow analysis.

The specific heat capacity: according to the thermoelacticity, the elastic properties, the heat capacity, and thermal expansion coefficient are correlated [10]. However, for C-S-H hydration product, the contribution of heat energy to its elastic behaviour can be neglected, meaning that the specific heat at constant volume (C_v) can be assumed equal to the specific heat capacity per unit volume (C_p) [2, 10]. Therefore, the effective heat capacity per unit volume (C_p^{eff}) can be derived by

$$C_p^{eff} = \left\langle C_p^r \right\rangle \approx C_v^{eff} \tag{2}$$

where C_p^r is the specific heat capacity of phase *r* in the nanostructure of the C-S-H. The calculated results of the effective thermal conductivity and specific heat capacity of the inner and outer C-S-H are also given in Table 1 (values in the parenthesis). The results are in good agreement with the previous results reported in [2]. Eqs. (1) and (2) can be also used for calculation of the effective thermal properties of the cement paste microstructure. The thermal properties of C-S-H phases (inner and outer) are taken from the analysis on the nanostructure of C-S-H as described earlier. The thermal properties of other phases are written in Table 1.

4. Experimental *vs* numerical results

An example of the results from the model for *w/c*=0.3 at 0.65 degree of reaction in terms of temperature gradient and the heat flux gradient is shown, respectively, in Figure 2a and b. In Figure 3, the obtained results in terms of the effective thermal conductivity are compared to the results from recent studies in the literature [11-15] for *w/c* ratios of 0.3 and 0.4 at different hydration time. It should be noted that the experimental results are collected only for saturated cement paste samples, and that the data is not necessarily correspondent to the same type of cement. Despite the observable scatter in the data obtained from the literature, the simulation lies within acceptable margins in regard to experimental data. In the same figure, a

comparison is also made between the simulation results and some few data in the literature [12, 13, 16] in terms of the specific heat capacity per mass unit of cement paste. The specific heat capacity per unit mass is calculated in accordance with the calculated density by the model using the discretized REV microstructure. The measurement of thermal properties of the exact cement type simulated in the present paper is still an ongoing process, and cannot yet be communicated herein.

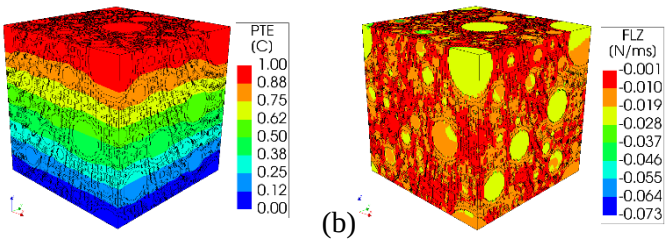

(a) (b)

Figure 2. (a) nodal temperature gradient (PTE), (b) heat flux gradient in z direction (FLZ)

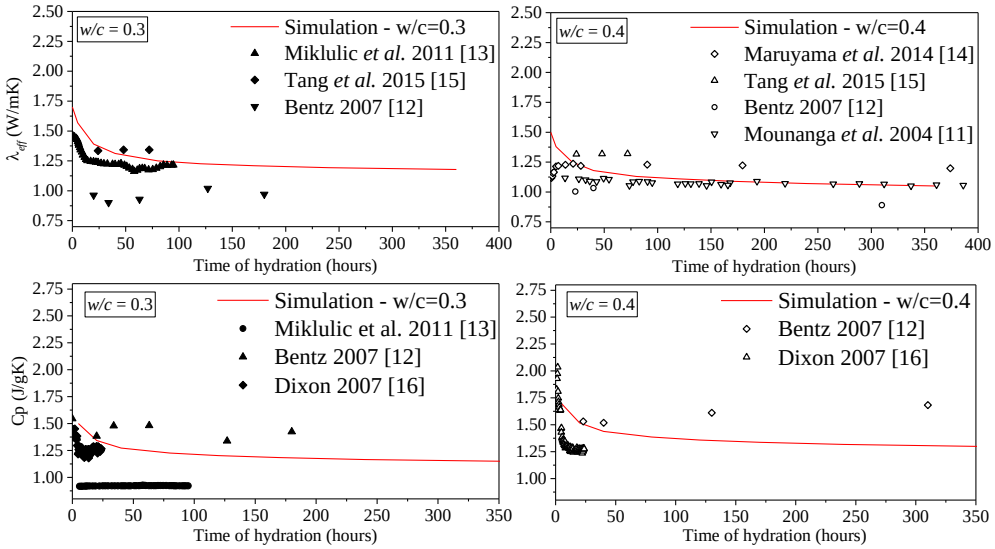

Figure 3. Comparison between the experimental and numerical results

6. Conclusion

The primary focus was on the evolution of the thermal conductivity and the specific heat capacity. The thermal properties obtained based on the nanostructure of C-S-H (both inner and outer) are in good agreement with the results in the literature. Despite the experimental results from the literature for cement paste being highly scattered, the obtained results are in an acceptable margin, providing grounds to the feasibility of the proposed methodology.

Acknowledgements

This work was financially supported by: Project POCI-01-0145-FEDER-007457 (CONSTRUCT - Institute of R&D in Structures and Construction) and by project POCI-01-0145-FEDER-007633 (ISISE), funded by FEDER funds through COMPETE2020 - Programa Operacional Competitividade e Internacionalização (POCI), and by national funds through FCT - Fundação para a Ciência e a Tecnologia. FCT and FEDER (COMPETE2020) are also

acknowledged for the funding of the research project IntegraCrete PTDC/ECM-EST/1056/2014 (POCI-01-0145-FEDER-016841). The financial support of COST Action TU1404 through its several networking instruments is also gratefully acknowledged.

References

[1] Miguel Azenha, Rodrigo Lameiras, Christoph de Sousa, and Joaquim Barros, *Application of air cooled pipes for reduction of early age cracking risk in a massive RC wall.* Engineering Structures, 2014. **62-63**: p. 148-163.
[2] Mohammad Javad Abdolhosseini Qomi, Franz-Josef Ulm, and Roland J. M. Pellenq, *Physical Origins of Thermal Properties of Cement Paste.* Physical Review Applied, 2015. **3**(6): p. 064010.
[3] Josephus Thomas Jr, Robert R Frost, and Richard D Harvey, *Thermal conductivity of carbonate rocks.* Engineering Geology, 1973. **7**(1): p. 3-12.
[4] Frank M. Etzler and Pamela J. White, *The heat capacity of water in silica pores.* Journal of Colloid and Interface Science, 1987. **120**(1): p. 94-99.
[5] Patrick A Bonnaud, Hegoi Manzano, Ryuji Miura, Ai Suzuki, Naoto Miyamoto, Nozomu Hatakeyama, and Akira Miyamoto, *Temperature dependence of nanoconfined water properties: application to cementitious materials.* The Journal of Physical Chemistry C, 2016. **120**(21): p. 11465-11480.
[6] Salvatore Torquato, Thomas M Truskett, and Pablo G Debenedetti, *Is random close packing of spheres well defined?* Physical review letters, 2000. **84**(10): p. 2064.
[7] Monica Skoge, Aleksandar Donev, Frank H. Stillinger, and Salvatore Torquato, *Packing hyperspheres in high-dimensional Euclidean spaces.* Physical Review E, 2006. **74**(4): p. 041127.
[8] Guang Ye, *Experimental study and numerical simulation of the development of the microstructure and permeability of cementitious materials*. 2003: PhD Thesis. TU Delft, Delft University of Technology.
[9] Klaas Van Breugel, *Simulation of hydration and formation of structure in hardening cement-based materials*. 1991: TU Delft, Delft University of Technology.
[10] Tulio Honorio, Benoit Bary, and Farid Benboudjema, *Thermal properties of cement-based materials: Multiscale estimations at early-age.* Cement and Concrete Composites, 2018. **87**: p. 205-219.
[11] Pierre Mounanga, Abdelhafid Khelidj, and Guy Bastian, *Experimental study and modelling approaches for the thermal conductivity evolution of hydrating cement paste.* Advances in cement research, 2004. **16**(3): p. 95-103.
[12] DP Bentz, *Transient plane source measurements of the thermal properties of hydrating cement pastes.* Materials and Structures, 2007. **40**(10): p. 1073.
[13] Dunja Mikulić, Bojan Milovanović, and Ivan Gabrijel, *Analysis of thermal properties of cement paste during setting and hardening*, in *Nondestructive Testing of Materials and Structures*. Springer. p. 465-471. 2013.
[14] Ippei Maruyama and Go Igarashi, *Cement reaction and resultant physical properties of cement paste.* Journal of Advanced Concrete Technology, 2014. **12**(6): p. 200-213.
[15] S. W. Tang, E. Chen, H. Y. Shao, and Z. J. Li, *A fractal approach to determine thermal conductivity in cement pastes.* Construction and Building Materials, 2015. **74**: p. 73-82.
[16] John C Dixon, *The shock absorber handbook*. 2008: John Wiley & Sons.